



**Mechanism of controlled integration of ZnO nanowires using pulsed-laser-induced chemical deposition**

Journal:	<i>Nanoscale</i>
Manuscript ID	NR-COM-08-2018-006890.R1
Article Type:	Communication
Date Submitted by the Author:	10-Dec-2018
Complete List of Authors:	Liu, Zhikun; South China University of Technology, Materials Science and Engineering Liu, Siyu; Purdue University, Industrial Engineering School Wu, Wenzhuo; Purdue University, School of Industrial Engineering Liu, C. Richard; Purdue University, Industrial Engineering; Purdue University

# Mechanism of controlled integration of ZnO nanowires using pulsed-laser-induced chemical deposition

Zhikun Liu<sup>a,b</sup>, Siyu Liu<sup>a</sup>, Wenzhuo Wu<sup>\*a,c</sup> and C. Richard Liu<sup>\*a,c</sup>

\* Corresponding author

<sup>a</sup> School of Industrial Engineering, Purdue University, West Lafayette, Indiana 47907, USA

E-mail: wenzhuowu@purdue.edu; liuch@purdue.edu

<sup>b</sup> School of Materials Science and Engineering, South China University of Technology, Guangzhou 510641, China

<sup>c</sup> Birck Nanotechnology Center, Purdue University, West Lafayette, Indiana 47907, USA

## Abstract

Laser-induced chemical deposition is an economical “grow-in-place” approach to produce functional materials. The lack of precise control over component density and other properties hinder the development of the method towards an efficient nanomanufacturing technology. In this paper, we provide a mechanism of direct pulsed-laser integration of ZnO nanowire seeding and growth on silicon wafers toward controlled density. Investigation of laser-induced ZnO nucleation directly deposited on a substrate suggested coverage percentage of nucleus particles was a function of instant available area, supplementing the classical nucleation theory for confined area deposition. A processing window was found in which ZnO nanowire only grew from the early deposited nucleated particles as seeds. Study on ZnO nanowire growth showed the process became transport limited over time, which was important for density-controlled nanowire growth integrated on nucleated seeds. The proposed mechanism provided guidance to integrate nanomaterials using laser-induced chemical deposition with controlled density and morphology.

## Introduction

Laser-induced chemical deposition<sup>1–8</sup> could synthesize and directly integrate (“grow-in-place”<sup>9</sup>) numerous functional nanomaterials without the needs to perform a series of procedures in the conventional nanomaterial growth processes (e.g., photolithography, seed deposition, lift-off, growth, etc). Moreover, each process in those conventional methods is time-consuming. On the contrary, laser technique provides a facile approach to grow and integrate nanomaterials

economically with micron-scale precision. The growth rate of nanotube<sup>1</sup> or nanowire<sup>2-6</sup> by the laser process was significantly higher than those by conventional methods. With rapid developments of parallel laser processing technology<sup>12-14</sup>, laser-induced chemical deposition is a promising method for scale-up production and integration of nanomaterials.

For practical applications, the density and other topological, geometric and functional properties of nanomaterials have strong impacts on the device performance. For example, the integration density of ZnO nanowires, a multi-functional nanomaterial of numerous application interests, can significantly affect the performance of related devices<sup>15-18</sup>. Therefore, the related fundamental understanding and technological capability in manufacturing is crucial and pressing<sup>9,19,20</sup> for advancing the laser processes.

Compared to the continuous-wave laser widely used for growing ZnO nanowires<sup>5-8</sup>, the use of pulsed-laser<sup>1-4</sup> could advance both the fundamental understanding and technological capability in integrating seeding and growing nanowires. This is because that pulsed laser has many more parameters available for control and tuning. Among others, many controlled variations of temperature can be generated at a duration of nano-, pico- femto-seconds by a pulsed-laser to help study and identify the values of multiple energy barriers in nucleation/growth which are important nanomanufacturing science for improving the productivity and quality of related materials.

Nevertheless, a pathway for the pulse-laser-induced chemical deposition and integration of nanomaterials (e.g., ZnO nanowires) and a fundamental understanding of related mechanism is lacking. Our work addressed these fundamental aspects and identified for the first time the mechanism for pulsed-laser-induced nucleation and growth of ZnO nanowires. In this paper, we report the controlled integration of ZnO nanowires by pulse-laser-induced chemical deposition and discuss the mechanism of it. The growth of nanowires was obtained on a more thermal conductive substrate (*i.e.*, Si wafer) without the need of an additional seed layer. The control over nanowire density was achieved by successfully decoupling the nucleation and crystal growth process. Based on that, we were also able to provide insights into nucleation and nanowire growth individually.

## Experimental

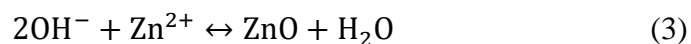
ZnO nanowires were deposited on silicon (0001) substrate induced by laser in a solution environment at room temperature. In this paper, the process of ZnO nucleation and nanowires growth was studied separately. High-frequency ytterbium-pulsed laser (1064 nm wavelength) was applied to initiate nucleation and induce nanowire growth. Laser energy was absorbed by the silicon substrate and thermally decomposed Hexamethylenetetramine (HMTA) and provided the  $\text{OH}^-$  ions for ZnO deposition.<sup>5</sup> HMTA and Zinc chloride ( $\text{ZnCl}_2$ ) were dissolved in 50 ml deionized water, with dilute nitric acid ( $\text{HNO}_3$ , pH=2.3) added to adjust the pH value of the solution. The solution for the nucleation process contained 6-22mM  $\text{ZnCl}_2$ , 66 mM HMTA and 1 ml dilute nitric acid; and the solution for nanowires growth contained 22 mM  $\text{ZnCl}_2$ , 12m M HMTA, and 6 ml-8ml dilute nitric acid. In the nanoparticle formation step, a silicon substrate with a size of 1 cm × 1 cm was immersed in the solution. Then the substrate was irradiated by a pulsed laser (6 W, 50 kHz) with a beam size of 200  $\mu\text{m}$  from the top through the aqueous solution, raising the temperature of the surrounding solution and initiating the reaction to form nanoparticles. If the heat were steadily generated and accumulated, the deposition of ZnO in the vicinity of the laser irradiation area would occur. To confine the deposition within the laser irradiation area, a moving plate was applied above the substrate to periodically block the laser irradiation and allowed the generated heat to dissipate. Specifically, the substrate was exposed to the laser for 3 s (on time) to induce chemical reaction and blocked for 20 s (off time) to prevent the heat accumulation. The total exposure time was 2 min for nanoparticles formation.

In the crystal growth step, the laser was operated at the same condition but the blocking plate was not used. Compared to nucleation, the crystal growth process generally required longer time to complete. Therefore, 1 hour steady laser (6 W) heating was applied for crystal growth. The nanowires grew upon the deposited nanoparticles in the first step. In order to eliminate the interference of additional nuclei on nanowire growth, acid was added to inhibit nucleation in this step. Scanning Electron Microscopy (SEM, Hitachi 4800 Field-Emission) was used to observe ZnO nanoparticles and nanowires arrays. Nanoparticle/nanowire density was measured by SEM at 3 different positions. At each position, about 200 nanoparticles/nanowires were counted for the density estimation. The nanowire length was measured by cross-sectional or tilted-view SEM. In general, the length of nanowires appeared to be uniform. 30 nanowires were measured for each sample to calculate the average length.

## Results and Discussion

### 1. Controlled integration of ZnO nanowire

Fundamental studies on the growth of ZnO nanowire by hydrothermal process have been conducted.<sup>21–24</sup> It was believed that the chemical reactions for growing ZnO nanowire by laser in solution were photothermal ones and similar to those by the hydrothermal process.<sup>5,6,8</sup> The energy of the laser was absorbed by the silicon substrate which caused the temperature of the solution to rising. The decomposition of HMTA was accelerated locally by laser heating which produced ammonia. By hydrolysis of ammonia, hydroxide ions were produced. The reaction between Zn ions and hydroxide ions lead to the formation of ZnO. The chemical reactions can be presented as follow<sup>23</sup>:



The controlled integration was performed in two steps: nucleation/integration of ZnO nanoparticles and the growth of the nanoparticles to be nanowires, as shown in Fig. 1a. In general, compared to crystal growth, crystal nucleation which dominant at high level of supersaturation requires shorter time to complete. Thus in the step of ZnO particle nucleation, laser irradiation chopped by a moving plate was employed to trigger the particle nucleation, while limiting the

growth of the particle. Whereas in the step of nanowire growth, steady laser irradiation was used to produce constant thermal energy, supporting the nanowire growth. Selective growth of ZnO nanomaterials was achieved by spin-coated seeding and electron beam lithography, photolithography or microstamp methods which required multiple steps.<sup>25</sup> In this work, the deposition area of ZnO was confined directly by the laser beam. ZnO nanowires with different density were integrated at the desired place of the silicon substrate without the need of spin-coated seed layer, which prevented the contamination of the ZnO on the unwanted region. Fig. 1 b1, b2 and Fig. 1 b3, b4 show the SEM pictures of ZnO deposition after nanoparticle nucleation and after nanowire growth respectively. The deposited spot areas of ZnO nanoparticles and nanowires were all around 200  $\mu\text{m}$  in diameter, the same as the size of the laser beam. The densities of integrated nanowire were determined by the density of the nanoparticles. When the density of nanoparticle was  $4 \times 10^8 \text{cm}^{-2}$ , free-standing nanowires of the same density were formed. The nanowires were 4  $\mu\text{m}$  in height with a diameter of 800 nm, as shown in Fig.1 b4, c4. The nanowires had a clear hexagonal structure, indicating a single crystalline wurtzite crystal structure. When the density reduced to  $1 \times 10^7 \text{cm}^{-2}$ , as the distances between particle increased, many of the nanowires grew laterally along the substrate (see Fig.1 c1, c2). If the density rose to  $1 \times 10^{10} \text{cm}^{-2}$ , a densely packed ZnO nanowire was obtained (see Fig.1 c6), forming a continuous thin film. The results were distinct from those in the early reports on the laser-induced deposition of ZnO in which only isolated nanowires were produced.<sup>5,6</sup> By the laser process reported here, the diameter of integrated nanowires ranged from 200 nm to 800 nm and the length ranged from 200 nm to 4  $\mu\text{m}$ , depending on the processing conditions. The two-step laser-induced chemical deposition of ZnO nanowire not only can integrate nanomaterials with controlled density, but also provide unique opportunities to acquire clearer understanding about nucleation and its influence on crystal growth.

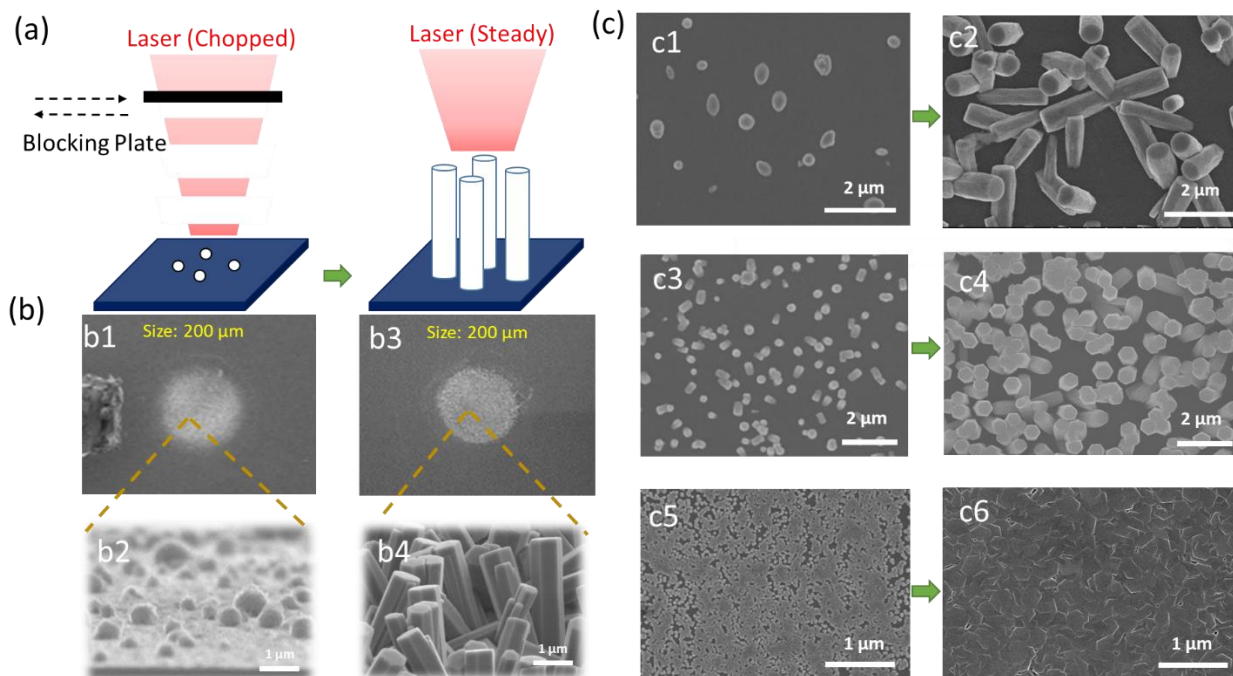


**Figure 1. Controlled integration of ZnO nanowire** (a) Schematic illustration of the experimental setup. (b) SEM pictures of ZnO deposition by laser-induced chemical deposition: (b1) (b2) integrated nanoparticles after laser-induced nucleation (b3) (b4) integrated nanowires after laser-induced nanowire growth. (c) SEM pictures of controlled integration of nanowire: (c1)(c2) in low density, (c3)(c4) in medium density, (c5)(c6) high density.

## 2. Nanoparticles nucleation induced by laser

During the step of nucleation/integration of ZnO nanoparticle, the substrate was under laser irradiation for 30 s and blocked from irradiation for 2 min. Laser heating effect caused the formation of hydroxide ions. The 2 min laser off time helped to prevent the accumulation of excessive hydroxide ions and heat which leading to ZnO deposition in the vicinity of the laser beam. This is different from the conventional hydrothermal method in which the whole solution was continuously heated, making the kinetics of nucleation harder to control. Although laser irradiation with higher power can promote the ZnO nucleation, it can also result in too much hydroxide ions and delocalized the deposition. Therefore laser power was kept constant (6 W) in the studies of nanoparticle density control.

The dependence of particle density on precursor concentration and time were studied. We found once the density of the particle was higher than  $10^8 \text{ cm}^{-2}$ , agglomeration of nanoparticles occurred. The agglomeration phenomenon suggested as the precursor concentration was raised for higher particle density, homogeneous nucleation above the substrate also took place during the particle formation process. The agglomeration would interfere with the nanowire growth process. Here we used a small amount (1 ml) of the dilute acid (pH=2.3) to inhibit the homogeneous nucleation while allowed the heterogeneous nucleation on a silicon substrate to occur. Therefore, nanoparticles with higher density could be formed without any particle agglomeration. By increasing the concentration of  $\text{ZnCl}_2$  from 6 mM to 22 mM, the particle density can vary in a large range, from  $1 \times 10^7 \text{ cm}^{-2}$  to  $1 \times 10^{10} \text{ cm}^{-2}$ , as shown in Fig. 2a. At the same time, the particle size reduced from about 1  $\mu\text{m}$  to 100 nm as the concentration of  $\text{ZnCl}_2$  increased from 6 mM to 22 mM. The nucleation phenomenon could be explained according to classical theory: As the supersaturation increased (higher concentration of  $\text{ZnCl}_2$ ), the size of the critical nucleus was smaller, which resulted in smaller nanoparticle and the heterogeneous nucleation rate was higher, which lead to a higher density of nanoparticle.

The particle density gradually increased over time by laser-induced deposition. However, the increase rate gradually slowed down, which could not be explained by the classical nucleation model which only considers temperature, pressure, and concentration of precursors. For deposition by focused laser, chemical reaction was confined in a micron-scale area, and inside the area, the coverage percentage (ZnO deposition area/ confined reaction area) varied significantly over time. As shown in Fig.2b, the average coverage percentages were 53%, 65%, 71% and 81% after 40 s, 1 min, 1 min 20 s and 2 min laser irradiation respectively. Since the duration of laser irradiation was short (< 2 min), the changes in precursor concentration and temperature were believed to be minor. Therefore, the nucleation rate per available area was treated constantly. Here, a model was developed to describe the change of the area coverage percentage over time for laser-induced deposition in a confined area:

$$A * (1 - x) * R = A * \frac{dx}{dt}$$

where A is the reaction area under laser irradiation, R is 2D coverage area increase rate, defined as deposition area/ (time\*instant available area), and t represents time.  $x = \frac{n*S}{A}$  was defined as the

area coverage percentage, where  $n$  is the number of nanoparticles,  $S$  is the area of a nanoparticles. Therefore,

$$x = 1 - \exp(-R * t)$$

Fitting the formula by experiment data, the coverage percentage:  $x = 1 - \exp(-0.017 * t)$ , as plotted in Fig.2c. This model could explain the deceleration of the deposition rate that deviated from the prediction of the classical model. The deceleration was mainly attributed to the reduced instant available area over time. The model cannot describe the change of particle density over time unless the variation of particle size is known. In Fig. 2b, from 1 mins to 1 mins 20s, the average size of particle increased from 90 nm to 120 nm, whereas the average density decreased from  $1.2 \times 10^{10}/\text{cm}^2$  to  $8 \times 10^9/\text{cm}^2$ . It suggests that Ostwald ripening occurred simultaneously as the new deposition was made on the substrate, which was not considered in this model.

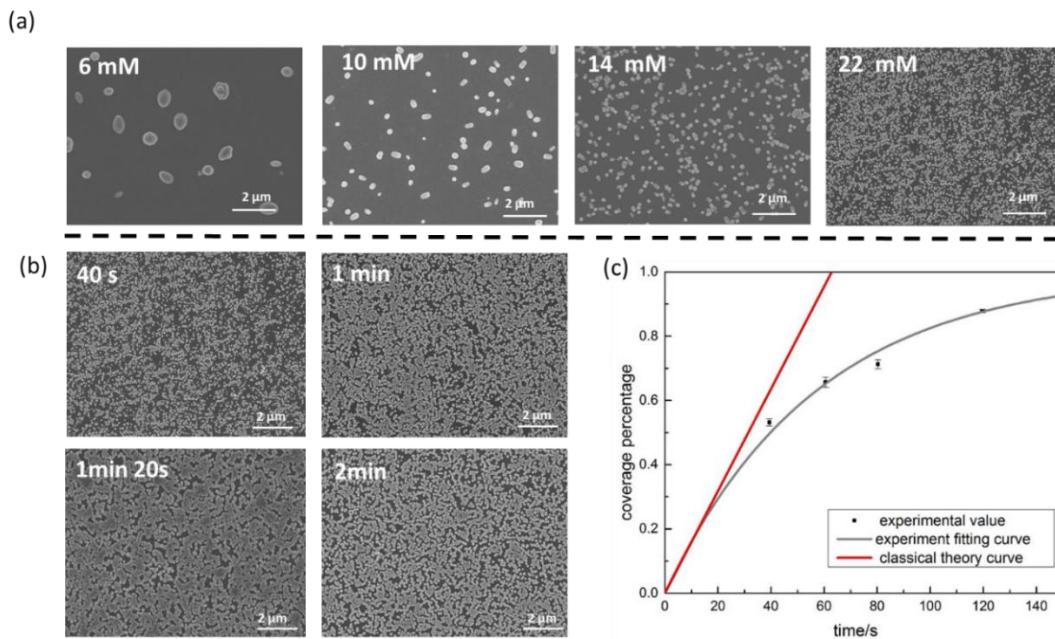


**Figure 2. Laser-induced ZnO nanoparticle nucleation/integration and density control** (a) SEM pictures of ZnO nanoparticles with different densities under different concentration of  $\text{ZnCl}_2$  6mM, 10mM, 14mM, and 22mM respectively. (b) SEM pictures of ZnO nanoparticles deposited in different deposition time 40s, 1min, 1min and 20s, and 2min. (c) The relationship between nanoparticle coverage percentage and deposition time.

### 3. The process window for crystal growth without additional nucleation

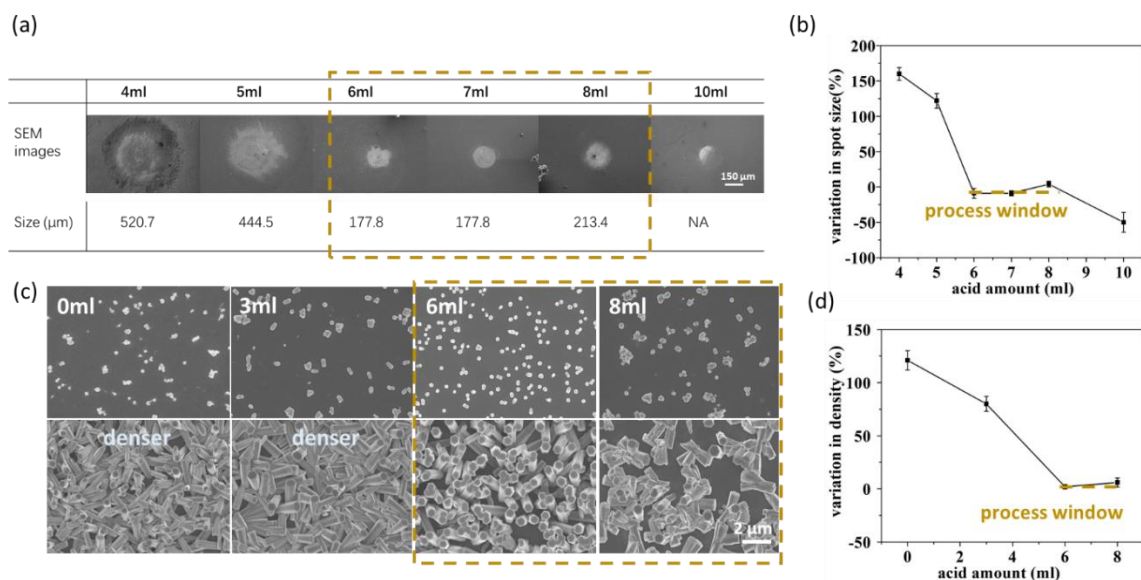


**Figure 3.** The process window for controlled integration of ZnO nanowire (a) SEM images of ZnO spots after 1 h crystal growth process with various amount of acid (pH=2.3) from 4ml to 10ml. (b) The corresponding line diagram shows the variation of the deposition area before and after nanowire growth in percentage. (c) SEM images of ZnO nanoparticles (top) and corresponding nanowires (bottom) with various amount of acid (pH=2.3) from 0 ml to 8 ml. (d) The corresponding line diagram shows the variation in the percentage of density in nucleation and nanowire growth processes. Error bars represent standard error range.

A critical step towards the controlled integration of nanowire is the growth of the nanowire from the particle while preventing nucleation of the new particle (inside/outside laser beam). Compared to the nucleation process, crystal growth required more time therefore steady laser irradiation was preferred for nanowire growth. However, constant laser irradiation increases the possibility of nucleation of ZnO on new sites. Previously, low conductivity of substrate (such as a polymer) was used to confine the heating zone and hinder nucleation on the area outside the laser beam.<sup>8</sup> The requirement on substrate limits the applicability of the laser method.

Our strategy is to add sufficient amount acid to the solution to reduce the supersaturation of ZnO (reduce the concentration of  $\text{OH}^-$  in reaction (3) in order to shift the reaction to the left), therefore, increases the energy barrier for nucleation. A processing window was defined, where nucleation was inhibited, and only crystal growth from the particle took place. Here, we found by adding acid within a specific range, ZnO deposition can also be localized on a relatively thermal conductive substrate, silicon. Fig.3a illustrates the deposition areas variation after nanowire growth for 1 h by

laser irradiation with different amount of the diluted acid ( $\text{HNO}_3$ ,  $\text{pH}=2.3$ ). The initial diameter of the ZnO nanoparticle deposition spot after laser-induced nucleation was around  $200\ \mu\text{m}$ . The SEM pictures in figure 3(a) show that the deposition area after crystal growth. When the amount of acid was less than 6 ml, the delocalization effect on deposition area was apparent. With 4 ml of acid, the deposition size became  $520\ \mu\text{m}$  in diameter. Moreover, with 5 ml of acid, the deposition size was  $440\ \mu\text{m}$ . When the amount of acid fell in the window of 6ml-8ml (see Fig. 3b), the deposition size almost did not change. When the amount of acid exceeded 10 ml, the existing nanoparticle was partly dissolved, and the deposition area decreased. At this processing window, nanowires density kept the same with the initial nanoparticle density. The comparison between the original nanoparticle density and nanowires density after 1 h nanowires growth with different amount of acid was shown in Fig.3c. When 0-3 ml acid was added to the precursor, the density of nanowires increased comparing to original nanoparticle density, indicating additional nucleation inside the confined area. When acid was added in the range of 6-8 ml, the nanowires density was approximately the same as the original particle density, which means nucleation was effectively inhibited in this process window. In the range above 10 ml acid added, a large portion of ZnO particles was dissolved by the acid, and the comparison cannot be made. In sum, inside the processing window (6-8 ml of the acid), nanowire growth was decoupled from nucleation of ZnO in the region outside/inside the laser beam and nanowire with controlled density can be integrated selectively.

#### 4. Nanowire growth induced by laser

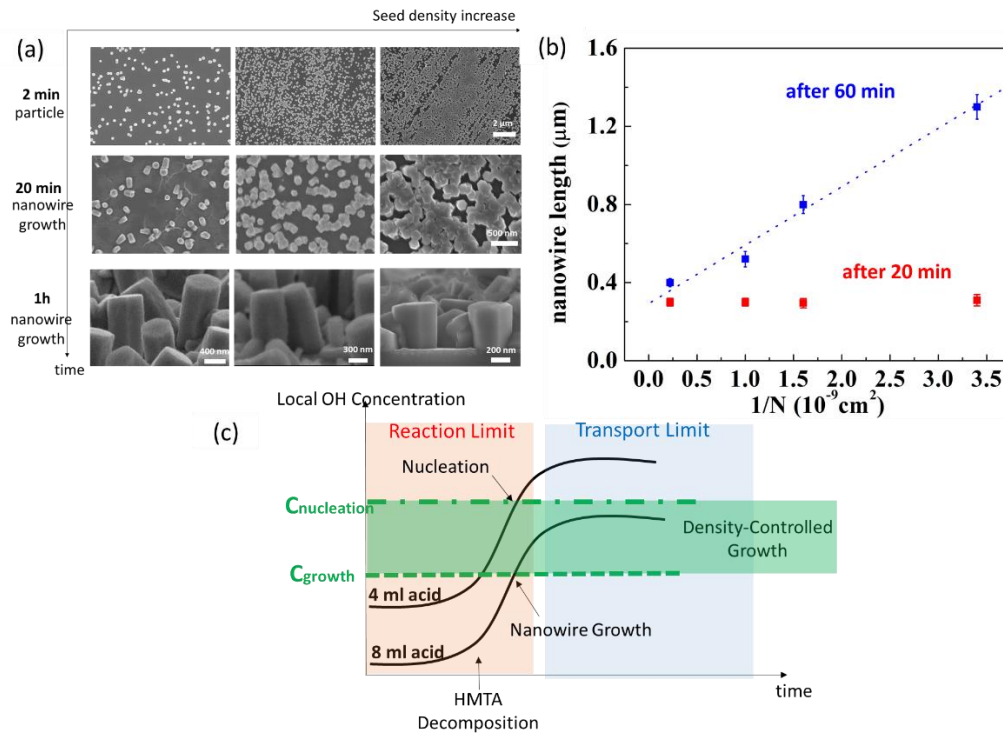


**Figure 4. Laser-induced crystal growth of ZnO nanowire** (a) SEM pictures of ZnO particles and nanowire after 2min, and nanowires after 20 min, 1 h respectively with various density. (b) The relationship between nanowire height and nanoparticle density after 20 min and 1 h respectively. Error bars represent standard error range. (c) change of local OH concentration over time.

Taking advantages of the processing window discussed above, nanowires could grow with the desired density. For the first time, the kinetics of laser-induced crystal growth can be studied with density as a controlled variable. According to the ZnO nanowire growth model proposed by Boercker *et al.*<sup>22</sup>, when the growth was mass transport limited, the nanowire growth rate was inversely proportional to the number density of it. Here, we investigated the nanowire growth in two stages: growth after 20 min and growth after 1 h, by exploring the relationship between nuclei density and nanowire length. The results (8 ml of the acid was added) are shown in Fig. 4a. At the beginning or 20 mins of laser irradiation, the length of crystals grown from nanoparticles with different densities was almost the same. However, after 1 hour of laser irradiation, it was apparent that the nanowire grown from loose nanoparticle were longer and larger. Nanoparticles with average densities of  $2.9 \times 10^8/\text{cm}^2$ ,  $6.4 \times 10^8/\text{cm}^2$ ,  $10.2 \times 10^8/\text{cm}^2$  and  $49.6 \times 10^8/\text{cm}^2$  were investigated. After 20 mins of laser irradiation, the average heights of the nanowires were all around  $0.3 \mu\text{m}$ , independent on the nuclei density. After 1 hour of laser irradiation, the heights of

nanowires were 1.3 $\mu\text{m}$ , 0.8 $\mu\text{m}$ , 0.5 $\mu\text{m}$ , and 0.4  $\mu\text{m}$  respectively. The nanowire height scales as  $1/N$  ( $N$  is the area density of nanowire), as shown in Fig. 4b. According to the model proposed by Boercker *et al.*, the nanowire height-density relationship suggests a laser-induced growth rate of ZnO was limited by chemical reaction at first, and then by mass transport from the bulk solution. Laser heating induced HMTA decomposition and rise of hydroxide ions locally. The supply of HMTA from the bulk to reaction zone was sufficient to keep up with the HMTA consumption. As the diffusion layer of HMTA increased, the supply of HMTA became inadequate, and the growth of ZnO nanowire was mass transport limited. We propose that the mass transport limited growth mode is essential for preventing nucleation on new sites during laser-induced crystal growth, as was illustrated in Fig. 4c. The insufficient mass transport kept the  $\text{OH}^-$  ions from accumulating excessively. When 8 ml diluted acid was added to the solution, the initial release of  $\text{OH}^-$  helped the local  $\text{OH}^-$  concentration to exceed the critical value for crystal growth. Moreover, nanowires began to grow from the existing nanoparticles. As the  $\text{OH}^-$  ions in the laser reaction spot accumulated locally, the inadequate precursor supply prevented the local  $\text{OH}^-$  concentration to exceed the critical value for nucleation of ZnO. This ensured the maintenance of crystal growth while inhibiting the nucleation. The proposed theory can explain the crystal growth window as discussed earlier. When less diluted acid was added to the solution (4 ml for example), the concentration of  $\text{OH}^-$  exceeded the critical value for nucleation before the reaction became transport limited. Subsequently, the size of the deposition/integration area and the density of nanowires increased as shown in Fig. 3. In this study, the objective is to reveal the mechanism of control integration. Thus the experimental setting was not optimized (relatively large amount of acid was used for example) to demonstrate the high growth rate by the laser process shown in previous reports<sup>1,6</sup>. The average growth rate demonstrated in this study (0.4~4 $\mu\text{m}/\text{h}$ ) was still higher than that by the conventional non-laser method (about 0.25  $\mu\text{m}/\text{h}$ <sup>22</sup>).

## Conclusion

By laser-induced chemical deposition, ZnO nanowires were selectively integrated onto a silicon wafer with controlled density. The control over nanowire density was realized by decoupling the nanowire growth process from ZnO nucleation on new sites. The discussed mechanisms associated with laser induced chemical deposition are expected to provide important guidance towards potential cost-effective production and integration of various nanomaterial systems<sup>26</sup>.

**Acknowledgment:** The project was partially supported by NSF (CMMI) Grant 1663214.

Note: Some of the ideas in this paper are covered by a patent pending.

**Reference:**

- 1 Z. Liu and C. Richard Liu, *Manuf. Lett.*, 2013, **1**, 42–45.
- 2 Z. Liu and C. R. Liu, *J. Micro Nano-Manufacturing*, , DOI:10.1115/1.4026546.
- 3 Z. Liu and C. R. Liu, *Proc. Inst. Mech. Eng. Part N J. Nanoeng. Nanosyst.*, 2013, **228**, 66–72.
- 4 Z. Liu, Z. Cao, B. Deng, Y. Wang, J. Shao, P. Kumar, C. R. Liu, B. Wei and G. J. Cheng, *Nanoscale*, 2014, **6**, 5853–8.
- 5 J. Yeo, S. Hong, M. Wanit, H. W. Kang, D. Lee, C. P. Grigoropoulos, H. J. Sung and S. H. Ko, *Adv. Funct. Mater.*, 2013, **23**, 3316–3323.
- 6 J. Bin In, H.-J. Kwon, D. Lee, S. H. Ko and C. P. Grigoropoulos, *Small*, 2014, **10**, 741–9.
- 7 J. Yeo, S. Hong, W. Manrotkul, Y. D. Suh, J. Lee, J. Kwon and S. H. Ko, *J. Phys. Chem. C*, 2014, **118**, 15448–15454.
- 8 J. Yeo, S. Hong, G. Kim, H. Lee, Y. D. Suh, I. Park, C. P. Grigoropoulos and S. H. Ko, *ACS Nano*, 2015, **9**, 6059–68.
- 9 M. Kwiat, S. Cohen, A. Pevzner and F. Patolsky, *Nano Today*, 2013, **8**, 677–694.
- 10 J. A. Liddle and G. M. Gallatin, *ACS Nano*, , DOI:10.1021/acsnano.5b03299.
- 11 H. Lee, W. Manrotkul, J. Lee, J. Kwon, Y. D. Suh, D. Paeng, C. P. Grigoropoulos, S. Han, S. Hong, J. Yeo and S. H. Ko, *ACS Nano*, 2017, **11**, 12311–12317.
- 12 S. Hasegawa, H. Ito, H. Toyoda and Y. Hayasaki, *Opt. Express*, 2016, **24**, 18513.
- 13 A. Gillner, M. Jüngst and P. Gretzki, in *Advanced Solid State Lasers*, OSA, Washington, D.C., 2015, p. AF3A.5.
- 14 M. Silvennoinen, J. Kaakkunen, K. Paivasaari and P. Vahimaa, *Opt. Express*, 2014, **22**, 2603.
- 15 X. D. Wang, J. Zhou, C. S. Lao, J. H. Song, N. S. Xu and Z. L. Wang, *Adv. Mater.*, 2007, **19**, 1627–1631.
- 16 W. Z. Wu, X. N. Wen and Z. L. Wang, *Science*, 2013, **340**, 952–957.
- 17 C. H. Liu, J. A. Zapien, Y. Yao, X. M. Meng, C. S. Lee, S. S. Fan, Y. Lifshitz and S. T.

- Lee, *Adv. Mater.*, 2003, **15**, 838–841.
- 18 R. H. Zhang, E. B. Slamovich and C. A. Handwerker, *Nanotechnology*, 2013, **24**, 195603.
- 19 S. E. Skrabalak and Y. Xia, *ACS Nano*, 2009, **3**, 10–15.
- 20 X. Liu, Y.-Z. Long, L. Liao, X. Duan and Z. Fan, *ACS Nano*, 2012, **6**, 1888–1900.
- 21 K. Govender, D. S. Boyle, P. B. Kenway and P. O'Brien, *J. Mater. Chem.*, 2004, **14**, 2575–2591.
- 22 J. E. Boercker, J. B. Schmidt and E. S. Aydil, *Cryst. Growth Des.*, 2009, **9**, 2783–2789.
- 23 Y. G. Wei, W. Z. Wu, R. Guo, D. J. Yuan, S. Das and Z. L. Wang, *Nano. Lett.*, 2010, **10**, 3411.
- 24 J. J. Cheng, S. M. Nicaise, K. K. Berggren and S. Gradečak, *Nano Lett.*, 2016, **16**, 753–759.
- 25 B. Weintraub, Z. Zhou, Y. Li and Y. Deng, *Nanoscale*, 2010, **2**, 1573–87.
- 26 Z. Y. Lin, Y. Zhao, C. J. Zhou, R. Zhong, X. Wang, Y. H. Tsang, and Y. Chai, *Scientific Reports*, 2015, **5**, 18596.